

p-Nitroanisole/Pyridine and p-Nitroacetophenone/Pyridine Actinometers Revisited: Quantum Yield in Comparison to Ferrioxalate

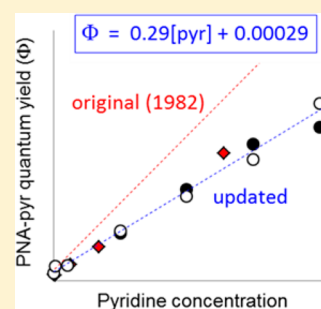
Juliana R. Laszakovits,[†] Stephanie M. Berg,[‡] Brady G. Anderson,[‡] Jessie E. O'Brien,[‡] Kristine H. Wammer,[‡] and Charles M. Sharpless^{*,†,‡,‡}

[†]Department of Chemistry, University of Mary Washington, Fredericksburg, Virginia 22401, United States

[‡]Department of Chemistry, University of St. Thomas, St. Paul, Minnesota 55105, United States

S Supporting Information

ABSTRACT: Chemical actinometry is often used to measure irradiance in environmental photochemistry. Two widely adopted actinometers are p-nitroanisole/pyridine (PNA-pyr) and the related but less popular p-nitroacetophenone/pyridine (PNAP-pyr). We report that PNA-pyr predicts systematically lower (−29%) photon irradiance than the well-characterized ferrioxalate actinometer. Thus, quantum yields previously determined using PNA-pyr should be correspondingly lower. Experiments at various pyridine concentrations produced an updated equation for the pyridine (pyr) dependence of the PNA-pyr quantum yield: $\Phi = 0.29[\text{pyr}] + 0.00029$. Additionally, we present a standard molar absorption spectrum of PNA for future use. A comparison between PNA-pyr and PNAP-pyr suggests the previously reported PNAP-pyr quantum yield is also too high. Preliminary results suggest a suitable equation for the PNAP-pyr system: $\Phi = 7.4 \times 10^{-3}[\text{pyr}] + 1.1 \times 10^{-5}$.



INTRODUCTION

Photodegradation is a well-recognized fate of aquatic contaminants, and photolysis rates depend critically on the irradiance at the water surface, measured in W m^{-2} or as photon irradiance, $\text{einstains cm}^{-2} \text{s}^{-1}$, where one einstein is one mole of photons. For environmental photochemistry, it is essential to quantify the irradiance so that experimental photolysis rates can be interpreted in terms of fundamental parameters, such as quantum yields¹ or fluence-based rate constants^{2,3} needed to model photochemical kinetics.

Two methods are common for determining irradiance: radiometry and actinometry. Radiometers typically use photodiodes and offer convenience and speed, especially when coupled with wavelength selection for spectroradiometry. However, they are relatively expensive, require regular calibration, are prone to damage if submerged for in situ measurements, and are unreliable in photoreactors with multiple lamps or irregular geometry, where light impinges from multiple angles. In contrast, actinometry is inexpensive and adaptable to many situations and thus finds frequent use. An actinometer is a light-sensitive chemical solution with known absorption and reaction quantum yield,^{4,5} the moles of reactant lost or product formed per einstein absorbed. Actinometry involves measuring the reaction rate and calculating irradiance from the actinometer's absorption and quantum yield.⁴

Dulin and Mill discuss desirable properties of actinometers for solar photochemistry,⁶ such as sensitivity at similar wavelengths to the reaction of interest and amenability to analysis over the same time scale. In practice, the stringency of

these requirements depends on how accurately the spectral distribution of the radiation is quantified and the available equipment. For example, identical time scales are unnecessary if radiometric monitoring and correction can be calibrated to actinometer reaction rates.⁷ Nonetheless, actinometry is most reliable when it meets the stated conditions. Dulin and Mill introduced two actinometers based on photonucleophilic substitution of excited state nitrobenzene derivatives by pyridine.⁶ Variation of the pyridine concentration allows adjustment of the quantum yields, providing access to a broad range of experimental time scales.

Since the original paper, the actinometers, p-nitroanisole/pyridine (PNA-pyr) and p-nitroacetophenone/pyridine (PNAP-pyr), have been widely adopted by environmental photochemists. Of the two, PNA-pyr is more extensively used; a literature search for this article found 80 instances of its use compared to 24 for PNAP-pyr. However, neither system's quantum yield (Φ) has been independently validated, and there are reasons to question the reported values. For example, Dulin and Mill determined Φ relative to the o-nitrobenzaldehyde actinometer, but recently Galbavya et al. concluded that its quantum yield should be lowered from the commonly accepted value of 0.505 to 0.41.⁸ This suggests that values of Φ reported by Dulin and Mill are at least 23% too large. Our experience with different actinometers agrees with this, and it led us to

Received: November 3, 2016
Revised: November 23, 2016
Accepted: November 28, 2016
Published: November 28, 2016

revisit the PNA-pyr actinometer by comparison with ferrioxalate,⁹ an exceedingly well-characterized actinometer that has been recommended for use as a laser power meter calibration standard.¹⁰ Its quantum yield has been validated at many wavelengths by various techniques,^{4,11,12} and potential errors and limitations have been explicitly delimited.^{13–15}

Here, we compare the photon irradiance determined by ferrioxalate and PNA-pyr at several wavelengths and revisit the pyridine concentration dependence of the PNA-pyr quantum yield. We find the original values of Φ for PNA-pyr are too large and suggest a revised equation for the pyridine concentration dependence. We also provide a molar absorption spectrum of PNA recommended for use by photochemists. A limited set of experiments comparing PNAP-pyr with PNA-pyr indicates that the original equation for the PNAP-pyr actinometer quantum yield is also in error, and we present an updated equation for that system.

EXPERIMENTAL SECTION

Comparative Ferrioxalate and PNA-pyr Actinometry.

Ferrioxalate actinometry used 0.02 M ferrioxalate in 0.05 M H₂SO₄. PNA-pyr actinometry used 10 μ M PNA in either 10, 12.5, or 15 mM aqueous pyridine, and PNAP-pyr actinometry used 15 μ M PNAP in 15 mM pyridine. More details on actinometer properties and preparation can be found in the [Supporting Information](#) (Sections S.1. and S.2).

Experiments were conducted in duplicate or triplicate using 5 mL of actinometer in a quartz test tube (1 cm i.d.) or between 1 and 3 mL in a 1 cm quartz cuvette. The container and volume had no discernible effect on the relative irradiance determined by the two actinometers. Irradiation times for PNA were sufficient to achieve at least 15% removal, which was measured by HPLC ([Supporting Information](#)). Ferrioxalate was run sequentially or concurrently with PNA under identical conditions to minimize errors associated with lamp fluctuations, and Fe(II) production was determined using phenanthroline ([Section S.2](#)).

Most experiments were conducted with a 300 W Xe lamp, a cold mirror, a series of short-pass filters (500, 450, and 400 nm; Edmund Optics), and narrow bandpass filters (~10–20 nm fwhm) or a broadband UG11 colored glass filter (280–400 nm range) for wavelength selection ([Figure S4](#)). Further details are provided in [Section S.2](#). Conditions were such that the irradiance was spatially uniform across the sample face to within 10% as verified by either radiometer (IL1700 with SED005 sensor and W-diffuser, International Light) with sensors masked to 1 cm aperture or a spectroradiometer with a 6.9 mm aperture (ILT550, International Light). Beam divergence was small enough that the irradiance at the back of the sample was within 5% of that at the face. Three to five experiments were conducted with each bandpass filter.

Photon Irradiance Calculations. PNA-pyr works as a pseudo-first-order actinometer, and HPLC peak areas were used to determine a first-order rate constant (k' , s⁻¹), from which the photon irradiance, $E_{p,tot}^0$ (einsteins cm⁻² s⁻¹) was calculated (eqs 1–4). Initial rates were used, $k'[\text{PNA}]_0$ (where $[\text{PNA}]_0$ is the initial PNA molarity), rather than the first-order limiting expression because at our PNA concentrations the numerator in eq 1 differs from the limit at zero absorbance by up to 12%, depending on the experimental wavelength. Here, $E_{p,\lambda}^0$ is the spectral photon irradiance (einsteins cm⁻² s⁻¹ nm⁻¹), ϵ_λ is the PNA molar absorption coefficient at each wavelength (M⁻¹ cm⁻¹), l is the optical path length (1 cm), Φ

is the PNA quantum yield (mol einstein⁻¹) calculated using eq 3,⁶ $\Delta\lambda$ is the wavelength resolution (1 nm), ρ_λ is the relative spectral photon irradiance ([Section S.2](#)), and $[\text{pyr}]$ is the pyridine molarity. Because identical sample containers were used for both actinometers, the container reflectance (ca. 2.5%) was not accounted for since it cancels out in the irradiance ratios used to compare the actinometers. Summations in eqs 1 and 2 were from 280 to 400 nm, where PNA absorption overlapped the lamp emission.

$$k'[\text{PNA}]_0 = 1000\Phi \frac{\sum_\lambda E_{p,\lambda}^0 (1 - 10^{-\epsilon_\lambda [\text{PNA}]_0}) \Delta\lambda}{l} \quad (1)$$

$$E_{p,\lambda}^0 = E_{p,tot}^0 \rho_\lambda \quad (2)$$

$$\Phi = 0.44[\text{pyr}] + 0.00028 \quad (3)$$

$$E_{p,tot}^0 = \frac{k'[\text{PNA}]_0 l}{1000\Phi \sum_\lambda \rho_\lambda (1 - 10^{-\epsilon_\lambda [\text{PNA}]_0}) \Delta\lambda} \quad (4)$$

Ferrioxalate is a zero-order actinometer and absorbs all the radiation ([Figure S1](#)), so the photon irradiance was determined using eq 5, where $\Delta A/\Delta t$ is the change in absorbance at 510 nm over time (cm⁻¹ s⁻¹), ϵ_{510} is the molar absorption coefficient of the Fe(II)-phenanthroline complex at 510 nm (11,100 M⁻¹ cm⁻¹),⁴ d is a factor accounting for dilution of sample in colorimetric reagent, and $\Phi_{\text{Fe(II)}}$ is the quantum yield for Fe(II) formation, taken as 1.25 mol einstein⁻¹ (280 nm < λ < 400 nm).⁴ Ferrioxalate's quantum yield is reported to decrease from 1.25 to 1.2 between 280 and 400 nm,⁴ but that variation is too small to affect the present results.

$$E_{p,tot}^0 = \frac{(\Delta A/\Delta t) dl}{1000\epsilon_{510} \Phi_{\text{Fe(II)}}} \quad (5)$$

Pyridine Concentration Dependence of Φ . Experiments to evaluate the pyridine dependence of Φ used a range from 0 to 25 mM pyridine, 30 μ M PNA or PNAP, and a broadband xenon lamp (Atlas Suntest CPS+). More detail is provided in [Section S.2](#).

RESULTS AND DISCUSSION

PNA-pyr Comparison to Ferrioxalate. [Figure 1](#) shows ratios of photon irradiance determined using PNA-pyr to those determined with ferrioxalate ($R_{p/F}$). All data are provided in [Tables S1 and S2](#). Consistently, PNA-pyr predicted a lower irradiance than ferrioxalate ($0.61 \leq R_{p/F} \leq 0.84$). Within the 95% confidence intervals ([Figure 1](#)), the ratio appears to be wavelength independent, consistent with the original report.⁶ However, the value at 313 nm appears to be somewhat high. At this wavelength, pyridine in our solutions absorbed approximately 5% of the radiation, and excited state pyridine may slightly alter the reaction mechanism. Using all the wavelengths yields an average ratio of 0.71 ± 0.09 , indicating the reported PNA-pyr quantum yield is too large by the inverse of this factor.

The overestimation of Φ by Dulin and Mill is at least in part related to their reference actinometer, o-nitrobenzaldehyde (o-NB). A recent report⁸ suggests that its quantum yield is 0.41 rather than 0.505 (used by Dulin and Mill), which implies that Φ for PNA-pyr is lower than originally reported by a factor of at least 0.81. Additionally, Morales et al. pointed out some years back¹⁶ that the reaction product of o-NB actinometry, o-nitrosobenzoic acid, strongly absorbs light above 300 nm. If not

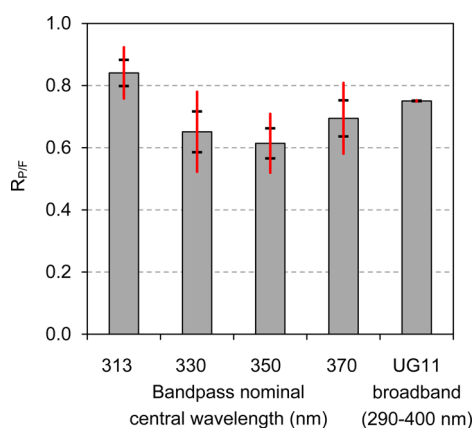


Figure 1. Ratio of photon irradiance determined by PNA-pyr to that determined by ferrioxalate ($R_{P/F}$) for each bandpass filter. Standard deviations (black bars) and 95% confidence intervals (red bars) are results from three or four experimental trials. All data and further details about the experimental errors can be found in the SI.

accounted for, irradiances calculated using o-NB may be too low because light screening from the product slows the actinometer photolysis. Though the reasons for the over-estimation of Φ by Dulin and Mill are not known, the present results suggest that PNA-pyr quantum yields should be reduced by a factor of 0.71.

Pyridine Dependence of PNA-pyr Quantum Yield.

Additional experiments were performed using a wide range of pyridine concentrations to re-evaluate the pyridine dependence of Φ . These experiments employed a broadband Xe lamp and used PNA both as received and after recrystallization. The results are shown alongside Dulin and Mill's in Table 1 and in Figure 2. Recrystallization had no effect.

Because the irradiation conditions here differ from those in Dulin and Mill, the rate constants have a different absolute dependence on pyridine concentration (Figure 2). This instrumental effect can be accounted for in both data sets to derive an equation for the pyridine dependence of Φ corrected

Table 1. Pyridine Concentration Dependence of PNA Loss Rate Constants Measured by Dulin and Mill (ref 6, Table I) and in this work^a.

| Dulin and Mill (1982) | | | this work | | |
|-----------------------------------|----------------------------|---------------------------|-----------------------------------|----------------------------|---------------------------|
| [pyr] (mM) | k' (min^{-1}) | C (min^{-1}) | [pyr] (mM) | k' (min^{-1}) | C (min^{-1}) |
| 0 | 7.83×10^{-4} | 2.80 | 4.85 ^b | 9.00×10^{-3} | 3.73 |
| 0.100 | 7.00×10^{-4} | 2.16 | 9.70 ^b | 1.72×10^{-2} | 3.78 |
| 1.20 | 2.00×10^{-3} | 2.48 | 14.6 ^b | 2.57×10^{-2} | 3.85 |
| 3.31 | 4.07×10^{-3} | 2.34 | 19.4 ^b | 2.89×10^{-2} | 3.28 |
| 12.4 | 1.54×10^{-2} | 2.68 | 0 | 1.52×10^{-3} | 5.42 |
| | | | 0.097 ^c | 2.76×10^{-3} | 8.55 ^d |
| | | | 0.97 ^c | 2.95×10^{-3} | 4.17 |
| | | | 4.85 ^c | 9.45×10^{-3} | 3.91 |
| | | | 9.70 ^c | 1.59×10^{-2} | 3.50 |
| | | | 14.6 ^c | 2.28×10^{-2} | 3.41 |
| | | | 19.4 ^c | 3.33×10^{-2} | 3.78 |
| average C (min^{-1}) | | 2.50 | average C (min^{-1}) | | 3.88 |

^aAlso provided are values of C , the instrumental parameter defined by eqs 6 and 7 and calculated using eq 3 for Φ (ref 6). ^bUsing unrecrystallized PNA. ^cUsing recrystallized PNA. ^dOutlier value of C as determined by Dixon's Q -test, not included in the average.

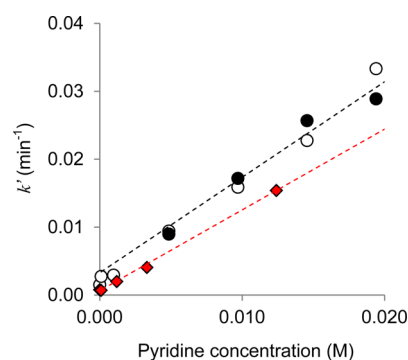


Figure 2. Pyridine concentration dependence of PNA loss rate constants: red diamond, Dulin and Mill, Table 1 (ref 6); black circle, this work, PNA used as received; white circle, this work, recrystallized PNA.

for consistency with ferrioxalate. The pseudo-first-order rate constant for PNA loss can be expressed as

$$k' = C\Phi \quad (6)$$

where

$$C = 3.6 \times 10^6 \frac{\sum_{\lambda} E_{p,\lambda}^0 (1 - 10^{-\epsilon_{\lambda}[\text{PNA}]_0}) \Delta\lambda}{I[\text{PNA}]_0} \quad (7)$$

Here, C (units, min^{-1}) is an instrumental constant dependent on the path length, lamp emission spectrum, and PNA concentration and absorption spectrum. From the rate constants in Table 1 and Dulin and Mill's equation for Φ (eq 3), eq 6 can be used to calculate associated values of C (Table 1). As expected, C is roughly constant with pyridine concentration within each set of experiments, so an average is applied in the ensuing analysis. The average C value was adjusted by the factor of 0.71 (eq 8) indicated by the ferrioxalate results, and rate constants from Table 1 were used in eq 9 to obtain ferrioxalate-adjusted values of Φ for each pyridine concentration.

$$C_{\text{corr}} = C/0.71 \quad (8)$$

$$\Phi = \frac{k'}{C_{\text{corr}}} \quad (9)$$

Figure 3 shows the resulting data and the best fit line (eq 10), which predicts lower Φ values than eq 3 by a factor of 0.81 at 1 mM pyridine and 0.67 at 15 mM pyridine, typical of concentrations encountered in the literature.

$$\Phi_{\text{PNA}} = 0.29[\text{pyr}] + 0.00029 \quad (10)$$

Pyridine Dependence of PNAP-pyr Quantum Yield.

We also re-examined the PNAP-pyr quantum yield by comparison to PNA-pyr in experiments excluding the wavelength dependence. Detailed methods and results are in the Supporting Information. A 46% lower irradiance was predicted by PNAP-pyr using Dulin and Mill's original quantum yield relative to PNA-pyr with the corrected quantum yield (eq 10). Experiments with variable pyridine concentrations were then used with the approach described above to derive an updated equation for the PNAP-pyr quantum yield (eq 11). Though it predicts much lower quantum yields than reported by Dulin and Mill, its intercept is very small, consistent with the original report.

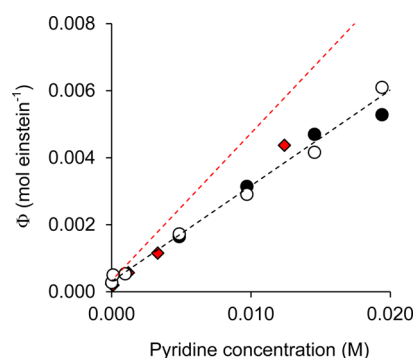


Figure 3. Pyridine concentration dependence of PNA-pyr photolysis quantum yield, Φ , calculated from rate constants in Table 1 and adjusted for agreement with ferrioxalate using eq 9 and the approach detailed in the text. Red dashed line is Dulin and Mill's eq 3 (ref 6). Black circle is from rate constants determined in this work using PNA as received. White circle is from rate constants determined in this work using recrystallized PNA. Red diamond is Dulin and Mill, Table 1 (ref 6). The best fit line to the data (black dashed line) is $\Phi = 0.29[\text{pyr}] + 0.00029$, $r^2 = 0.9854$, where $[\text{pyr}]$ is the molar concentration of pyridine.

$$\Phi_{\text{PNAP}} = 0.0074[\text{pyr}] + 1.1 \times 10^{-5} \quad (11)$$

Recommendations. We recommend eq 10 for future use in PNA-pyr actinometry and that previously reported quantum yields determined using PNA-pyr be lowered by a factor of 0.71. Furthermore, we recommend a standard PNA molar absorption spectrum, which is provided in the Supporting Information with experimental details given in the Supporting Information. Finally, we recommend preliminary use of eq 11 for PNAP-pyr actinometry and that results from that actinometer be corroborated with additional independent measurements.

■ ASSOCIATED CONTENT

● Supporting Information

The Supporting Information is available free of charge on the ACS Publications website at DOI: 10.1021/acs.estlett.6b00422.

Actinometer information, solution preparation, analytical details, lamp emission spectra, data for Figure 1, details for variable pyridine experiments, details of PNAP-pyr experiments, and molar absorption spectra of PNA and PNAP. (PDF)

Molar absorption spectrum of PNA. (XLSX)

■ AUTHOR INFORMATION

Corresponding Author

*Phone: (540) 654-1405. E-mail: csharp@umw.edu.

ORCID

Charles M. Sharpless: 0000-0003-3520-7418

Notes

The authors declare no competing financial interest.

■ ACKNOWLEDGMENTS

The authors acknowledge support from NSF awards CBET-1132207, CBET-1335711, OCE-1333-26 and thank Hugh Anderson and Marlene Caceres for experimental assistance.

■ REFERENCES

- (1) Schwarzenbach, R. P.; Gschwend, P. M.; Imboden, D. M. Direct Photolysis. In *Environmental Organic Chemistry*, 2nd ed.; Wiley and Sons, 2003; Chapter 15.
- (2) Sharpless, C. M.; Linden, K. G. Experimental and model comparisons of low- and medium-pressure Hg lamps for the direct and H₂O₂ assisted UV photodegradation of N-nitrosodimethylamine in simulated drinking water. *Environ. Sci. Technol.* **2003**, *37*, 1933–40.
- (3) Stefan, M. I.; Bolton, J. R. Fundamental approach to the fluence-based kinetic and electrical energy efficiency parameters in photochemical degradation reactions: polychromatic light. *J. Environ. Eng. Sci.* **2005**, *4*, 13–18.
- (4) Montalti, M.; Credi, A.; Prodi, L.; Gandolfi, M. T. Chemical Actinometry. In *Handbook of Photochemistry*, 3rd ed.; CRC: Boca Raton, FL, 2006; Chapter 12a and references therein.
- (5) Kuhn, H. J.; Braslavsky, S. E.; Schmidt, R. Chemical actinometry (IUPAC technical report). *Pure Appl. Chem.* **2004**, *76*, 2105–2146.
- (6) Dulin, D.; Mill, T. Development and evaluation of sunlight actinometers. *Environ. Sci. Technol.* **1982**, *16*, 815–820.
- (7) Wei-haas, M. L.; Chin, Y.-P. A fluence-based method for the direct comparison of photolysis kinetics under variable light regimes. *Environ. Sci. Technol. Lett.* **2015**, *2*, 183–187.
- (8) Galbavy, E. S.; Ram, K.; Anastasio, C. 2-Nitrobenzaldehyde as a chemical actinometer for solution and ice photochemistry. *J. Photochem. Photobiol., A* **2010**, *209*, 186–192.
- (9) Hatchard, C. G.; Parker, C. A. A new sensitive chemical actinometer. II. Potassium ferrioxalate as a standard chemical actinometer. *Proc. R. Soc. London, Ser. A* **1956**, *235*, 518–536.
- (10) Demas, J. N.; Bowman, W. D.; Zalewski, E. F.; Velapoldi, R. A. Determination of the quantum yield of the ferrioxalate actinometer with electrically calibrated radiometers. *J. Phys. Chem.* **1981**, *85*, 2766–2771.
- (11) Bolton, J. R.; Stefan, M. I.; Shaw, P.-S.; Lykke, K. R. Determination of the quantum yields of the potassium ferrioxalate and potassium iodide–iodate actinometers and a method for the calibration of radiometer detectors. *J. Photochem. Photobiol., A* **2011**, *222*, 166–169.
- (12) Goldstein, S.; Rabani, J. The ferrioxalate and iodide–iodate actinometers in the UV region. *J. Photochem. Photobiol., A* **2008**, *193*, 50–55.
- (13) Nicodem, D. E.; Cabral, M. L. P. F.; Ferreira, J. C. N. The use of 0.15 M potassium ferrioxalate as a standard chemical actinometer. *Mol. Photochem.* **1977**, *8*, 213–238.
- (14) Bowman, W. D.; Demas, J. N. Ferrioxalate actinometry: A warning in its correct use. *J. Phys. Chem.* **1976**, *80*, 2434–2435.
- (15) Kirk, A. D.; Namasivayam, C. Errors in ferrioxalate actinometry. *Anal. Chem.* **1983**, *55*, 2428–2429.
- (16) Morales, R. G. E.; Java, G. P.; Cabrera, S. Solar ultraviolet radiation measurements by o-nitrobenzaldehyde actinometry. *Limnol. Oceanogr.* **1993**, *38*, 703–705.